CORE
Metadata, citation and similar papers at core.ac.uk
Provided by VCU Scholars Compass

Virginia Commonwealth University
VCU Scholars Compass

Electrical and Computer Engineering Publications
Dept. of Electrical and Computer Engineering

2005

Efficacy of single and double SiNx interlayers on defect reduction in GaN overlayers grown by organometallic vapor-phase epitaxy

F. Yun
Virginia Commonwealth University

Y.-T. Moon
Virginia Commonwealth University

Y. Fu
Virginia Commonwealth University

See next page for additional authors

Follow this and additional works at: http://scholarscompass.vcu.edu/egre_pubs

Part of the Electrical and Computer Engineering Commons

Yun, F., Moon, Y. T., Fu, Y., et al. Efficacy of single and double SiNx interlayers on defect reduction in GaN overlayers grown by organometallic vapor-phase epitaxy. Journal of Applied Physics 98, 123502 (2005). Copyright © 2005 AIP Publishing LLC.

Downloaded from

http://scholarscompass.vcu.edu/egre_pubs/171

This Article is brought to you for free and open access by the Dept. of Electrical and Computer Engineering at VCU Scholars Compass. It has been accepted for inclusion in Electrical and Computer Engineering Publications by an authorized administrator of VCU Scholars Compass. For more information, please contact libcompass@vcu.edu.

Authors
F. Yun, Y.-T. Moon, Y. Fu, K. Zhu, U. Ozgur, H. Morkoç, C. K. Inoki, T.S. Kuan, Ashutosh Sagar, and R. M. Feenstra

This article is available at VCU Scholars Compass: http://scholarscompass.vcu.edu/egre_pubs/171

Efficacy of single and double SiN_x interlayers on defect reduction in GaN overlayers grown by organometallic vapor-phase epitaxy

F. Yun, Y. -T. Moon, Y. Fu, K. Zhu, Ü. Özgür, and H. Morkoç[a)]
Department of Electrical and Computer Engineering, Virginia Commonwealth University, Richmond, Virginia 23284

C. K. Inoki and T. S. Kuan
Department of Physics, University at Albany, State University of New York (SUNY), Albany, New York 12222

Ashutosh Sagar and R. M. Feenstra
Department of Physics, Carnegie Mellon University, Pittsburgh, Pennsylvania 15213

(Received 21 July 2005; accepted 7 November 2005; published online 16 December 2005)

We report on the growth of and evolution of defects in GaN epilayers having single- and double-layer SiN_x nanoporous insertion layers. The SiN_x was formed *in situ* in the growth chamber of an organometallic vapor-phase epitaxy system by simultaneous flow of diluted silane and ammonia. The GaN epilayers and SiN_x interlayers were grown on 6*H*-SiC substrates using three different nucleation layers, namely, low-temperature GaN, high-temperature GaN, and high-temperature AlN nucleation layers. X-ray-diffraction rocking curves and cross-sectional and plan-view transmission electron microscope analyses indicated that a nanoporous SiN_x layer can reduce the dislocations density in the GaN overgrown layer to $\sim 3\times 10^8$ cm^{-2} range; below this level the defect blocking effect of SiN_x would saturate. Therefore the insertion of a second SiN_x layer becomes much less effective in reducing dislocations, although it continues to reduce the point defects, as suggested by time-resolved photoluminescence measurements. The insertion of SiN_x interlayers was found to improve significantly the mechanical strength of the GaN epilayers resulting in a much lower crack line density. © *2005 American Institute of Physics*.
[DOI: 10.1063/1.2142074]

I. INTRODUCTION

Extensive research and development efforts expended in III-nitride materials over the past decades have enabled the commercialization of a variety of devices such as solar-blind ultraviolet (UV) photodetectors, lasers and light-emitting diodes, and modulation-doped field-effect transistors.[1] In spite of these developments, the full potential of GaN-based devices has yet to be realized due to the GaN material itself suffering from a high density of defects inherent to heteroepitaxy on foreign substrates necessitated by a lack of native GaN substrates. Further improvements in high-performance devices call for the reduction of performance degradation on which threading dislocations play a sizable role as they, at the very least, are capable of trapping point defects or forming complexes with them. Currently, the mainstream growth method for thin-film GaN material is organometallic vapor-phase epitaxy (OMVPE), which typically produces GaN layers with a dislocation density in the 10^9-10^{10} cm^{-2} range. Several techniques have been employed for dislocation reduction such as epitaxial lateral overgrowth (ELO),[2–6] TiN nanoporous network,[7–9] $Si_xAl_{1-x}N$ interlayer,[10] and SiN_x, nanomask.[11–14] Using a conventional ELO technique, the dislocation density can be reduced to the 10^5 cm^{-2} in the wing region and 10^8-10^9 cm^{-2} in the window region.

Compared to the conventional ELO approach, the use of an *in situ* prepared amorphous and nanoporous SiN_x layer has the advantage of maskless, one-step processing, and possible contamination associated with the *ex situ* lithography process in traditional ELO methods can be eliminated. The reduced feature sizes of the SiN_x network also facilitates nanometer-scale epitaxial lateral growth (nano-ELO) at the open pores, thereby considerably reducing the inhomogeneity between the wing and window regions commonly seen in the traditional ELO growth which has adverse effect on devices.

Recently, an order-of-magnitude reduction in the GaN dislocation density (down to 7×10^8 cm^{-2}) attributed to the use of a nanoporous SiN_x interlayer atop a low-temperature GaN (LT-GaN) nucleation layer on a 6*H*-SiC substrate was reported. It is known that a high-temperature GaN (HT-GaN) nucleation layer grown at ~ 1000 °C on SiC offers a better template than a low-temperature GaN layer (grown at ~ 550 °C) in terms of better crystalline quality and surface morphology. High-temperature AlN (HT-AlN) nucleation layers have even better quality for reducing crack density, due to closer lattice and thermal match to the 6*H*-SiC substrate. It is thus expected that the SiN_x nanoporous networks built on top of these high-temperature nucleation layers are likely to be superior to their LT-buffer counterparts in producing higher quality overgrown GaN layers. It is also possible that the insertion of a second or more SiN_x inter-

[a)]Author to whom correspondence should be addressed; electronic mail: hmorkoc@vcu.edu

 © 2005 American Institute of Physics

[This article is copyrighted as indicated in the article. Reuse of AIP content is subject to the terms at: http://scitation.aip.org/termsconditions. Downloaded to] IP: 128.172.48.58 On: Tue, 20 Oct 2015 14:36:51

layers may further block dislocations and or point defects from penetrating into the top layer, resulting in a superior quality GaN top layer.

In this paper, we report on the growth experiments and dislocation analyses with the adoption of SiN_x nanoporous interlayers on LT-GaN, HT-GaN, and HT-AlN nucleation layers and the comparison of their efficacy. Particular attention will be paid to which type of dislocations is more susceptible to blocking by these nanoporous interlayers. The utility of double SiN_x interlayers for dislocation reduction and surface crack improvement is also tested.

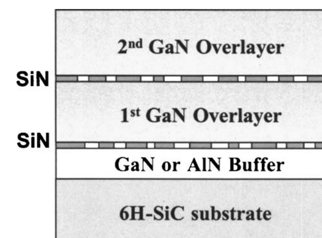

FIG. 1. Schematic diagram of the structure of GaN epitaxy by OMVPE on a 6*H*-SiC substrate. Three sets of samples were grown using LT-GaN, HT-GaN, and HT-A1N nucleation layers. On each nucleation layers, three samples were grown, namely, (1) GaN overlayer grown on nucleation layer without SiN_x (control sample); (2) GaN overlayer grown on single SiN_x interlayer; and (3) GaN overlayer grown with double SiN_x insertion.

II. EXPERIMENT

The investigated samples were grown on the Si face of *n*-type 6*H*-SiC (on-axis) substrates by OMVPE. The SiC substrates were thermally annealed in a hydrogen flow at 1700 °C, to remove the surface damage induced by mechanical polish and to attain a surface with biatomic steps. Trimethylgallium (TMGa) and trimethyaluminum (TMAl) were used as precursors for Ga and Al, and ammonia (NH_3) as nitrogen source during OMVPE growth of GaN and AlN nucleation layers.

Three sets of samples were grown using (1) LT-GaN nucleation layer at 560 °C; (2) HT-GaN nucleation layer at 950 °C; and (3) HT-AlN at 1090 °C. The thickness of the nucleation layers is ~100 nm. During the growth of nucleation layers and subsequent GaN overlayers, the chamber pressure was kept at 30 Torr, and the V/III ratio at 2000.

Immediately following the nucleation layer growth, the flow of TMGa (or TMAl in the case of AlN nucleation layer) was interrupted while keeping the NH_3 flow. Simultaneously, diluted silane (100 ppm) was fed into the chamber at a flow rate of 50 SCCM (standard cubic centimeter per minute) for 5 min to form a thin and discontiguous SiN_x nanoporous network. The subsequent GaN overlayer growth for all samples was carried out at 1030 °C. In each set of growth using LT-GaN, HT-GaN, or HT-AlN nucleation layers, three samples were prepared. The first sample had no SiN_x interlayer and served as a control sample. The second one had a single SiN_x interlayer on the nucleation layer. The third sample had two SiN_x layers, with the second one inserted after a 2-μm-thick GaN was grown on top of the first SiN_x. For this sample, the subsequent GaN overgrowth was carried out on the second SiN_x nanoporous network until the surface was fully coalesced and smooth. Figure 1 illustrates the schematics of the layer structures used in this paper. The GaN overlayers were unintentionally doped and were grown up to 8 μm in thickness.

The crystalline quality of the GaN overlayers was studied by high-resolution x-ray-diffraction (XRD) rocking curves using a Phillips X'Pert XRD diffractometer equipped with a four-crystal Ge (220) monochrometer. The relationship between epitaxy and dislocation structures was investigated by cross-sectional transmission electron microscopy (TEM). Plan-view TEM micrographs were also taken to determine accurately the density, distribution, and type of dislocations near the top GaN surface. Optical properties were studied by time-resolved photoluminescence (TRPL) measurements performed at room temperature, using a 45 ps resolution Hamamatsu streak camera. Pulsed (~100 fs) excitation density was kept at ~200 $\mu J/cm^2$ which is below the stimulated emission threshold to measure the decay times. The surface crack line density was examined using an optical microscope.

III. RESULTS AND DISCUSSION

The existence and morphology of a thin and nanoporous network of SiN_x using the above mentioned *in situ* deposition technique has been confirmed previously using scanning Auger microscopy (SAM) mapping. The SiN_x coverage on the GaN buffer was found to be highly dependent on the silane concentration, flow rate, and exposure time. For instance, 5% of silane flow for 5 min would result in a subsequent overgrowth of polycrystalline GaN, indicative of a complete coverage of SiN_x over the nucleation layer. As such, all the samples discussed here used the identical SiN_x deposition conditions optimized to produce a nanoporous network as evidenced by SAM.

TABLE I. Summary of the XRD FWHM data, TEM dislocation density, and crack density data for GaN overlayers grown with single- and double-layer SiN_x using low-temperature GaN nucleation layers.

Samples	GaN thickness (μm)	Crack denisty (mm^{-1})	XRD FWHM (arc min) (0002)	XRD FWHM (arc min) ($10\bar{1}2$)	TEM dislocation density (cm^{-2}) All types
No SiN_x	3.3	8.0	10.7	26.0	$\sim 6\times 10^9$
Single SiN_x	4.2	3.9	10.9	15.6	$\sim 4\times 10^9$
Double SiN_x	3.9	5.1	9.6	12.0	$\sim 1\times 10^9$

[This article is copyrighted as indicated in the article. Reuse of AIP content is subject to the terms at: http://scitation.aip.org/termsconditions. Downloaded to] IP: 128.172.48.58 On: Tue, 20 Oct 2015 14:36:51

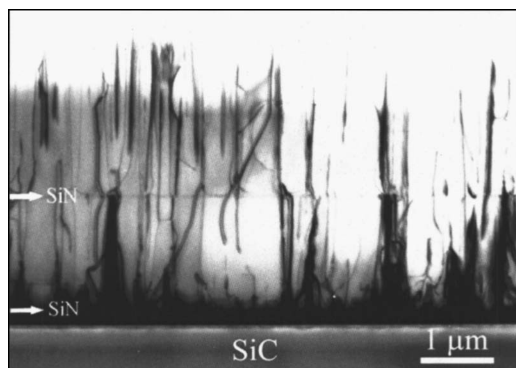

FIG. 2. Cross-sectional TEM micrograph of a GaN overlayer grown with the insertion of two SiN_x nanoporous interlayers, on a LT-GaN nucleation layer by OMVPE on a 6*H*-SiC substrate.

A. Effects of SiN_x in dislocation reduction

XRD rocking curve measurements were carried out for both the symmetric (0002) and asymmetric $(10\bar{1}2)$ reflections. Table I summarizes the first set of samples employing LT-GaN nucleation layers. The x-ray rocking curve full width at half maximum (FWHM) shows consistent improvement for the asymmetric $(10\bar{1}2)$ reflection with the use of single- and double-layer SiN_x. The $(10\bar{1}2)$ FWHM of 26.0 arc min for the control sample was reduced drastically to 15.6 arc min when a single-layer SiN_x was used, and to 12.0 arc min when double-layer SiN_x were inserted. The FWHMs of the (0002) reflection, however, remained roughly the same for the control sample (10.7 arc min), the single SiN_x (10.9 arc min), and the double SiN_x (9.6 arc min) samples. It is known that in wurtzite GaN crystals, the symmetric (0002) reflection is affected by the density of pure screw dislocations with Burgers vector $b=[0001]$, while the asymmetric $(10\bar{1}2)$ diffraction is most sensitive to edge-type $(b=1/3[11\bar{2}0])$ and mixed-type dislocations.[15] Accordingly, the x-ray-diffraction data shown in Table I suggest that the edge dislocation density has been effectively reduced by the use of a single-layer SiN_x, and was further filtered by a second layer of SiN_x.

Cross-sectional TEM images taken on this set of samples are consistent with the XRD data. Figure 2 shows a representative TEM micrograph of the sample with double SiN_x interlayers grown on a LT-GaN nucleation layer. Here the dislocation density is observed to reduce dramatically at the first SiN_x interlayer located at the interface between the LT-GaN nucleation layer and the GaN overlayer. The change in dislocation density at the second SiN_x layer is, however, not as pronounced as the first layer over the LT-GaN buffer. The cross-sectional TEM image from the control sample without the SiN_x layer also shows significant dislocation reduction at the LT-GaN/GaN overlayer interface. To detect the effects of SiN_x layers we thus have to rely on comparing the dislocation density observed at the top GaN overlayer (Table I). It is noted that plan-view images would allow more accurate determination of dislocation density. However, because of the high crack density in the GaN overlayers, we were not able to prepare plan-view TEM specimen from these samples. Nevertheless, cross-sectional TEM observations indicate that the total dislocation density is reduced by the first SiN_x layer and continues to be reduced by the second SiN_x layer to $\sim 1\times 10^9$ cm^{-2}.

X-ray diffraction is known to provide information on the average crystalline quality integrating over the total thickness of the film. Alternatively, TEM images are more useful in discerning the layer-specific dislocation structure. Based on a joint analysis of the XRD and TEM data in Table I, it is reasonable to infer that most of the blocked dislocations are edge type (or mixed type), not screw type. Electron-diffraction patterns taken from the GaN layers overgrown on SiN_x interlayer(s) reveal further that they are free of any *c*-axis tilt typically found over the wing regions in a traditional ELO process.[16] Similar behavior of SiN_x has been found previously in growths using sapphire substrates.

B. High-temperature versus low-temperature nucleation layers

The use of a low-temperature nucleation layer on SiC usually leads to inferior nucleation quality which in turn compromises the quality of the GaN overlayer. This is precisely why the XRD data in Table I show relatively broad FWHMs. In this context, the high-temperature GaN nucleation layer in and of itself offers higher crystalline quality. To suppress crack formation, AlN offers an advantage over GaN in having a thermal expansion coefficient closer to that of SiC. A HT-AlN nucleation layer has an additional benefit of closer lattice match to 6*H*-SiC substrate $(<1.0\%)$ than does GaN (3.5%). As such, we have grown additional two sets of GaN samples on top of HT-GaN and HT-AlN nucleation layers, respectively. Table II summarizes a set of three samples grown on HT-GaN nucleation layers, using a structure identical to that shown in Fig. 1.

It is evident from Table II that the FWHMs of x-ray rocking curves are much narrower than those grown using

TABLE II. Summary of the XRD FWHM data, TEM dislocation density, and crack density data for GaN overlayers grown with single- and double-layer SiN_x using high-temperature GaN nucleation layers.

Samples	GaN thickness (μm)	Crack denisty (mm^{-1})	XRD FWHM (arc min)		TEM dislocation density (10^8 cm^{-2})	
			(0002)	$(10\bar{1}2)$	Screw	Edge
No SiN_x	8.2	3.3	4.7	8.5	0.38	12
Single SiN_x	5.3	1.2	3.6	4.9	0.66	3.7
Double SiN_x	8.4	2.4	4.3	5.2	0.69	3.6

[This article is copyrighted as indicated in the article. Reuse of AIP content is subject to the terms at: http://scitation.aip.org/termsconditions. Downloaded to] IP: 128.172.48.58 On: Tue, 20 Oct 2015 14:36:51

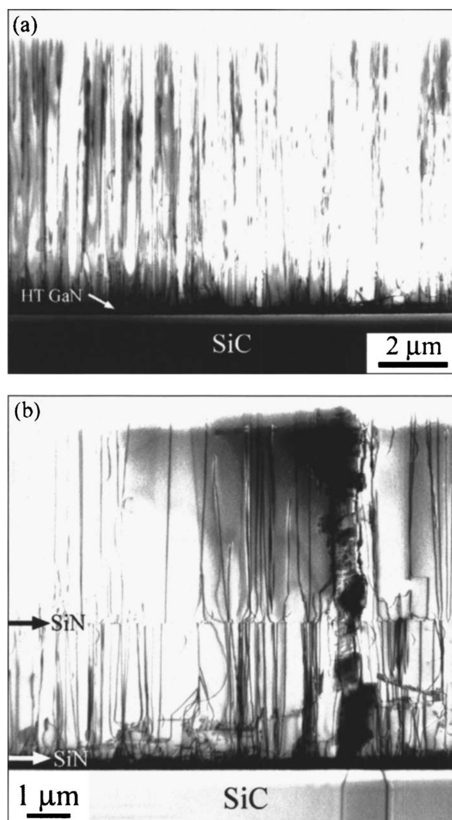

FIG. 3. Cross-sectional TEM micrographs of GaN overlayers grown on HT-GaN nucleation layers (a) without SiN_x (control sample), and (b) with double SiN_x interlayers, by OMVPE on 6*H*-SiC substrates.

LT-GaN nucleation layers, a strong indication that the crystalline quality becomes better when a HT-GaN nucleation layer is adopted. Similar to the samples grown on LT-GaN nucleation layers, the symmetric (0002) peak width stays roughly the same for the control sample (4.7 arc min) and the samples with either a single SiN_x layer (3.6 arc min) or double SiN_x layers (4.3 arc min). This suggests that SiN_x causes no significant changes in the screw dislocation density. In contrast, the FWHM of the asymmetric $(10\bar{1}2)$ peak decreases from 8.5 arc min for the control sample to 4.9 and 5.2 arc min for the single- and double-layer SiN_x samples, respectively. This indicates a clear reduction in the density of the edge- and mixed-type dislocations at the first SiN_xinterlayer.

TEM analyses provide direct microscopic evidence substantiating the XRD data. Displayed in Fig. 3 are the cross-sectional TEM micrographs of the control sample (without SiN_x) and the sample with double SiN_x layers, both on HT-GaN nucleation layers. In the control sample, most of the threading dislocations propagate from the nucleation layer vertically and reach straight to the top GaN surface. On the contrary, the cross-sectional image of Fig. 3(b) indicates that most threading dislocations emerging from a SiN_x nanoporous network (the first or second SiN_x interlayer) tend to bend and interact among themselves, leading to dislocation combinations. After about a half of a micrometer of overgrowth, the remaining dislocations resume their vertical configuration. Threading dislocations were also found to be

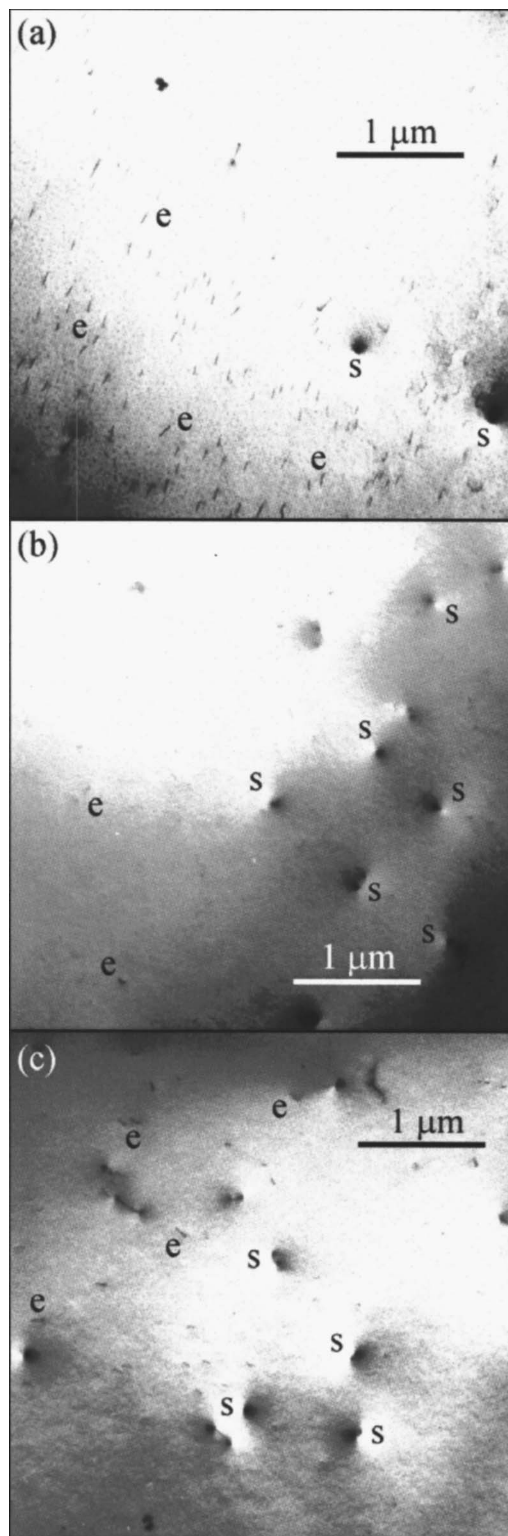

FIG. 4. Plan-view TEM micrographs of GaN overlayers grown on HT-GaN nucleation layers, (a) without SiN_x (control sample), (b) with a single SiN_x interlayer, and (c) with double SiN_x interlayers, by OMVPE on 6*H*-SiC substrates, "e" stands for edge-type dislocations and "s" screw-type dislocations.

blocked by terminating at the SiN_x porous layer. Our x-ray and TEM observations indicate that this blocking mechanism is most effective when the dislocation density is high, i.e., at the first SiN_x interlayer. When the average spacing between threading dislocations exceeds the porous network feature

[This article is copyrighted as indicated in the article. Reuse of AIP content is subject to the terms at: http://scitation.aip.org/termsconditions. Downloaded to] IP: 128.172.48.58 On: Tue, 20 Oct 2015 14:36:51

TABLE III. TRPL decay constants and amplitude ratios (at 200 $\mu J/cm^2$ excitation density) for GaN epitaxy thin films grown with single (*s*-SiN) and double (*d*-SiN) SiN layers, on LT-GaN, HT-GaN, and HT-AlN, and nucleation layers, respectively.

	LT-GaN nucleation layer			HT-GaN nucleation layer			HT-AlN nucleation layer		
	Control	*s*-SiN	*d*-SiN	Control	*s*-SiN	*d*-SiN	Control	*s*-SiN	*d*-SiN
τ_1 (ns)	0.04	0.09	0.10	0.04	0.16	0.10	0.13	0.20	0.29
τ_2 (ns)	0.15	0.18	0.29	0.54	0.45	0.85	0.32	0.45	0.77
A_2/A_1	0.03	0.27	0.61	0.04	0.30	0.62	0.06	0.42	0.38

size, e.g., at the second SiN_x interlayer, the blocking ceases to occur, since a total blocking requires multiple dislocations with a zero Burgers vectors sum terminating at the same location. As a result, a large portion of the threading dislocations has been filtered out by the first SiN_x interlayer, but not at the second interlayer.

Plan-view TEM measurements are highly desirable in dislocation analysis because they provide not only an accurate count of the dislocation density at the top GaN surface, but also the specific details of each dislocation type. Shown in Fig. 4 are the plan-view TEM micrographs taken for the three GaN samples grown on HT-GaN nucleation layers. The "end-on" screw-type dislocations (marked as "s") exhibit a strong, characteristic bright-dark contrast perpendicular to the imaging reflection vector. Such contrast is absent at the edge-type (marked as "e") dislocations. Direct counting of dislocations from the image in Fig. 4(a) indicates that the majority (>95%) of dislocations in the control sample are edge type (1.2×10^9 cm^{-2}). With the use of a single SiN_x interlayer [Fig. 4(b)], the edge dislocation density is reduced by a factor of about 3, to $\sim3.7\times10^8$ cm^{-2}. In Fig. 4(c) we found that a second SiN_x layer did not reduce any further the edge dislocation density ($\sim3.6\times10^8$ cm^{-2}).

Although the effect of SiN_x in dislocation reduction tends to saturate from single to double SiN_x, and with higher quality nucleation layers, improvements in terms of nonradiative recombination center density continue progressively from single to double SiN_x layers, and on the high-quality nucleation layers as well.

The TRPL decays for all the samples were well characterized by a biexponential decay function $A_1\exp(-t/\tau_1)+A_2\exp(-t/\tau_2)$. Table III summarizes the room-temperature TRPL decay constants and amplitude ratios[17] for the GaN samples grown with single and double SiN layers. From the table, it can be seen that for each type of nucleation layer used, the decay constants exhibit a trend of increase with the use of single SiN and double SiN layers, over the control sample. The amplitude ratio A_2/A_1 also increases with the same trend. The improvement can also be seen with the use of HT-AlN and HT-GaN nucleation layers compared to the LT-GaN nucleation layers. However, slight variations to the trend do exist. For example, for the HT-GaN nucleation layer case, the double SiN gives slightly smaller τ_1 (0.10 ns) than the single SiN sample (τ_1=0.16 ns), but they are still larger than the control sample, and the A_2/A_1 ratio has been significantly increased from 0.04 for the control, to 0.30 for the single SiN, and 0.62 for the double SiN samples. In fact, compared to the biexpoential decay times τ_1 and τ_2, the ratio of slow to fast decay amplitude A_2/A_1 is more pertinent to the relative importance of radiative decay. Thus a larger A_2/A_1 indicates increased radiative efficiency. The results in Table III strongly suggest that with the inclusion of a second SiN layer, the overgrown GaN shows improved radiative efficiency over the single SiN sample and the control sample. Therefore, the use of a second SiN layer is well justified.

The dislocation density for each type counted from the plan-view TEM micrographs is summarized in Table II. It is found that the screw-type dislocation density ($\sim$mid-10^7 cm^{-2} range) is already at least one order of magnitude lower than the edge-type in the control sample. This is typical for the OMVPE-grown GaN using GaN nucleation layers.[18] The density of screw-type dislocations is obviously at the range too low for the SiN_x nanoporous network to have an appreciable impact on. On the other hand, the edge-type dislocations at a much higher density were reduced from $\sim1.2\times10^9$ to $\sim3\times10^8$ cm^{-2} by the SiN_x interlayer. This $\sim3\times10^8$ cm^{-2} is presumably the low boundary for the SiN_x interlayer to act on dislocations.

The results of another set of samples using HT-AlN nucleation layers are summarized in Table IV. The trend in the x-ray FWHM of the (0002) reflection is nominally the same in that there is very little if any variation among the control sample (without SiN_x), the single SiN_x sample, and

TABLE IV. Summary of the XRD FWHM data, TEM dislocation density, and crack density data for GaN overlayers grown with single- and double-layer SiN_x using high-temperature AlN nucleation layers.

Samples	GaN thickness (μm)	Crack denisty (mm^{-1})	XRD FWHM (arc min)		TEM dislocation density (10^8 cm^{-2})	
			(0002)	$(10\bar{1}2)$	Screw	Edge
No SiN_x	8.2	3.3	4.7	8.5	0.38	12
Single SiN_x	5.3	1.2	3.6	4.9	0.66	3.7
Double SiN_x	8.4	2.4	4.3	5.2	0.69	3.6

[This article is copyrighted as indicated in the article. Reuse of AIP content is subject to the terms at: http://scitation.aip.org/termsconditions. Downloaded to] IP: 128.172.48.58 On: Tue, 20 Oct 2015 14:36:51

the double SiN_x sample. The FWHM of the $(10\bar{1}2)$ reflection remains almost unchanged for the single SiN_x sample (8.4 arc min) as compared to the control (7.9 arc min), but significantly reduced when the double SiN_x interlayers were employed (4.4 arc min). The plan-view TEM micrographs in Fig. 5 show a dislocation distribution quite different from that of GaN overlayers grown on HT-GaN nucleation layers. The populations of screw-type dislocations and edge-type dislocations are more or less comparable here for all samples, whereas the HT-GaN nucleation layer produces dominantly edge-type dislocations in the overlayers. This might be related to the different lattice and thermal mismatch conditions. Since the density of both types of dislocations in the control sample are already at or close to the low limit for the SiN_x layer to have any effect ($\sim 3\times 10^8$ cm^{-2}), we therefore observe no reduction (beyond the statistical scatter) of screw- or edge-type dislocations by the first or second SiN_x interlayer.

Even though the SiN_x interlayer cannot block individual dislocations, it can still bend them, particularly the edge dislocations. The bending allows dislocations to rearrange and/or line up into arrays so as to minimize their long-range strain fields. In Fig. 5(c) we observed such array formation facilitated by the double SiN_x layers. These edge dislocation arrays constitute subgrain boundaries and give rise to much less $(10\bar{1}2)$ peak broadening (4.4 arc min) as we have observed in Table IV. Thus, the commonly accepted proportional relationship between the dislocation density and the square of FWHM of asymmetric $(10\bar{1}2)$ peak[19] does not necessarily hold. This observation offers one possible mechanism for some conflicting results between XRD and TEM dislocation density occasionally seen in the literature.

To further explore the role of SiN_x on different nucleation layers, we compare the total dislocation density among the three control samples (without SiN_x) using LT-GaN, HT-GaN, and HT-AlN nucleation layers. As listed in Tables I, II, and IV there is a consistent decrease in the total dislocation density from 6×10^9 to 1.2×10^9 cm^{-2}, and to 7.3×10^8 cm^{-2}, when the respective nucleation layer is LT-GaN, HT-GaN, or HT-AlN. Expectedly, the use of high-temperature nucleation layers by themselves improves the crystalline quality of GaN overlayers largely due to better nucleation conditions in general, and due to smaller lattice and thermal mismatches for HT-AlN nucleation layers, in particular. From the data presented above, the efficacy of the SiN_x interlayer(s) in dislocation reduction proves to be significant on the LT-GaN nucleation layers and moderate on HT-GaN nucleation layers, but seems to saturate on the HT-AlN nucleation layers. This is easily understood since the better the control samples are, the less efficient SiN_x can filter threading dislocations.

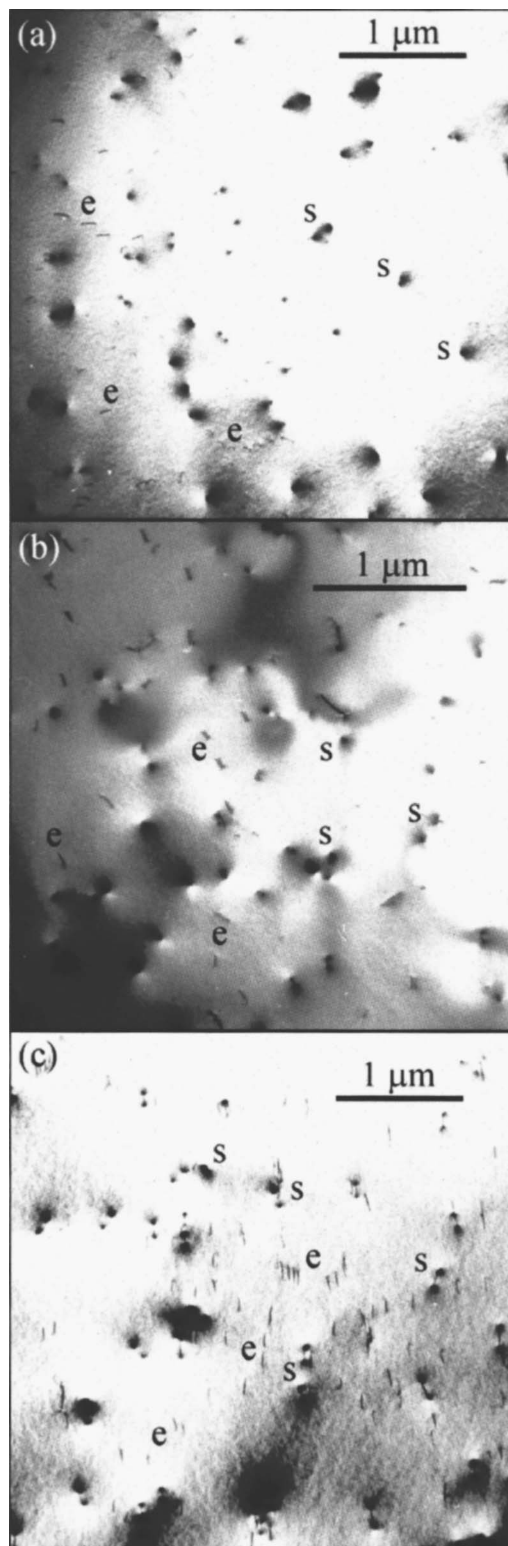

FIG. 5. Plan-view TEM micrographs of GaN overlayers grown on HT-AlN nucleation layers, (a) without SiN_x (control sample), (b) with a single SiN_x interlayer, and (c) with double SiN_x interlayers, by OMVPE on 6*H*-SiC substrates, "e" stands for edge-type dislocations and "s" screw-type dislocations. Most edge dislocations in (c) are observed to align into arrays.

C. Reduction of crack density by SiN_x, interlayers

In addition to defect reduction, an added benefit of SiN_x interlayers is the alleviation of surface cracks commonly encountered in GaN grown on SiC by OMVPE. For all the samples discussed in this paper, crack line densities are measured by opical microscopic images and are tabulated in Table I, II, and IV. Selected crack line images are shown in Fig. 6. For the set of samples with LT-GaN nucleation layer, the control GaN [Fig. 6(a)] has a highest crack density (8.0 mm^{-1}). With the insertion of a single SiN_x [Fig. 6(b)], the crack line density was reduced to 3.9 mm^{-1}. For the set

[This article is copyrighted as indicated in the article. Reuse of AIP content is subject to the terms at: http://scitation.aip.org/termsconditions. Downloaded to] IP: 128.172.48.58 On: Tue, 20 Oct 2015 14:36:51

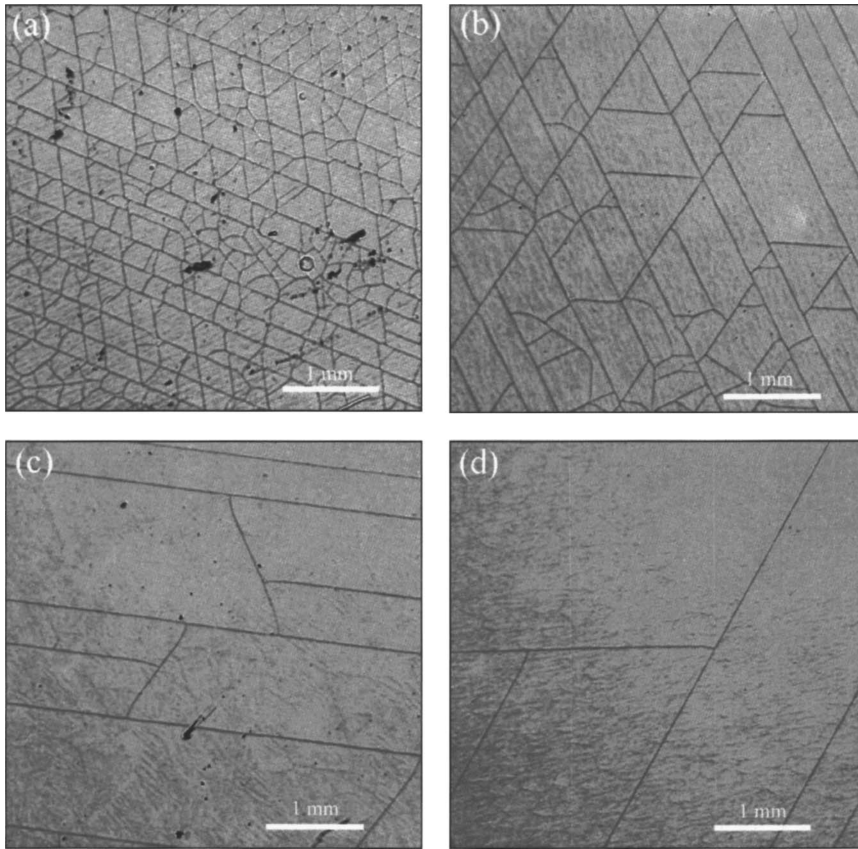

FIG. 6. Optical microscopic images showing crack lines on the OMVPE-grown GaN surface on (a) LT-GaN nucleation layer without SiN_x, (b) LT-GaN nucleation layer with single SiN_x, (c) HT-GaN nucleation layer with single SiN_x, and (d) HT-AlN nucleation layer with double SiN_x. All samples were grown on 6*H*-SiC substrates. The scale bars in all the images are 1 mm.

of samples with HT-GaN nucleation layers, with crack line density was reduced from 3.3 mm^{-1} for the control sample, to 1.2 mm^{-1} for the single SiN_x sample shown in Fig. 6(c). For the set of samples with HT-AlN nucleation layers, the use double SiN_x produces the lowest crack density of 0.7 mm^{-1} [Fig. 6(d)] wheareas for the single SiN_x sample it is 1.3 mm^{-1}. It is noted that the crack tends to increase with GaN thickness. In evaluating the beneficial crack reduction effect of HT-GaN and HT-AlN nucleation layers and the SiN_x interlayer we have to take into account the adverse GaN layer thickness effect. In Fig. 6(a)–6(d) the thickness increases from 3.3 to 7.4 μm while the crack density decreases from 8.0 to 0.7 mm^{-1}. Thus the combined advantages of using HT-AlN and double SiN_x layers in reducing crack density should be more than ten folds. Our observations clearly indicated that the porous thin SiN_x interlayer can serve to either release some thermal stress or decrease crack nucleation rate resulting in a crack reduction of roughly 30%–50% during the postgrowth cooling down to room temperature. We thus find that the SiN_x mitigates the cracking problem in GaN grown on SiC, and the use of multiple SiN_x layers may further enhance the mechanical strength and reduce the crack line density to an accepted level for device application.

IV. CONCLUSIONS

Single and double layers of thin and porous SiN_x have been inserted *in situ* before or during the growth of GaN epitaxial layers to serve as a mask to promote lateral growth. Dislocation reduction has been achieved to varying degrees depending on the nucleation layers used. SiN_x is found to be most effective in reducing the edge-type dislocations, bringing the total dislocation density down to $\sim 3 \times 10^8$ cm^{-2}. As the crystalline quality of GaN is improved using HT-nucleation layers, the efficacy of SiN_x in dislocation reduction tends to saturate, although it continues to improve the radiative recombination and carrier lifetimes which are closely associated with point defects. The use of a second SiN_x layer is found to be more effective in reducing the point-defect density than the threading dislocations. In addition to defect reduction, SiN_x is also useful in mitigating the surface crack problem commonly experienced in GaN grown on SiC substrates.

ACKNOWLEDGMENT

This work was supported by a Defense University Research Initiative on Nanotechnology (DURINT) program administered by the Office of Naval Research under Grant No. N00014-01-1-0715 (program monitor Dr. Colin Wood).

[1]H. Morkoç, *Nitride Semiconductors and Devices* (Springer, Berlin, 1999).
[2]T. S. Zhelva, O. -H. Nam, M. D. Bremser, and R. F. Davis, Appl. Phys. Lett. **71**, 2472 (1997).
[3]P. Gibart, Rep. Prog. Phys. **67**, 667 (2004).
[4]R. S. Q. Fareed, J. W. Yang, J. Zhang, V. Adivarahan, V. Chaturvedi, and M. A. Khan, Appl. Phys. Lett. **77**, 2343 (2000).
[5]A. M. Roskowski, E. A. Preble, S. Einfeldt, P. M. Miraglia, and R. F. Davis, J. Electron. Mater. **31**, 421 (2002).
[6]D. Kapolnek, S. Keller, R. Vetury, R. D. Underwood, P. Kozodoy, S. P. DenBaars, and U. K. Mishra, Appl. Phys. Lett. **71**, 1204 (1997).
[7]Y. Oshima, T. Eri, M. Shibata, H. Sunakawa, and A. Usui, Phys. Status Solidi A **194**, 554 (2002).
[8]F. Yun *et al.*, Phys. Status Solidi A **202**, 749 (2005).
[9]Y. Fu *et al.*, Appl. Phys. Lett. **86**, 043108 (2005).

[This article is copyrighted as indicated in the article. Reuse of AIP content is subject to the terms at: http://scitation.aip.org/termsconditions. Downloaded to] IP: 128.172.48.58 On: Tue, 20 Oct 2015 14:36:51

[10]T. Akasaka, T. Nishida, Y. Taniyasu, M. Kasu, T. Makimoto, and N. Kobayashi, Appl. Phys. Lett. **83**, 4140 (2003).
[11]S. Haffouz, B. Beaumont, P. Vennegues, and P. Gibart, Phys. Status Solidi A **176**, 677 (1999).
[12]T. Wang, Y. Morishima, N. Naoi, and S. Sakai, J. Cryst. Growth **213**, 188 (2000).
[13]S. Sakai, T. Wang, Y. Morishima, and Y. Naoi, J. Cryst. Growth **221**, 334 (2000).
[14]A. Sagar, R. M. Feenstra, C. K. Inoki, T. S. Kuan, Y. Fu, Y. T. Moon, F. Yun, and H. Morkoç, Phys. Status Solidi A **202**, 722 (2005).
[15]B. Heying, X. H. Wu, S. Keller, Y. Li, D. Kapolnek, B. P. Keller, S. P. DenBaars, and J. S. Speck, Appl. Phys. Lett. **68**, 643 (1996).
[16]S. Einfeldt, A. M. Roskowski, E. A. Preble, and R. F. Davis, Appl. Phys. Lett. **80**, 953 (2002).
[17]Ü. Özgür, Y. Fu, Y. T. Moon, F. Yun, H. Morkoç, and H. O. Everitt, J. Appl. Phys. **97**, 103704 (2005).
[18]V. Narayanan, K. Lorenz, W. Kim, and S. Mahajan, Appl. Phys. Lett. **78**, 1544 (2001).
[19]P. Gay, P. B. Hirsch, and A. Kelly, Acta Metall. **1**, 315 (1953).

[This article is copyrighted as indicated in the article. Reuse of AIP content is subject to the terms at: http://scitation.aip.org/termsconditions. Downloaded to] IP: 128.172.48.58 On: Tue, 20 Oct 2015 14:36:51